POLITECNICO DI TORINO
Repository ISTITUZIONALE

Static Response and Buckling Loads of Multilayered Composite Beams Using the Refined Zigzag
Theory and Higher-Order Haar Wavelet Method

Terms of use:

(Article begins on next page)

09 April 2024

Static response and buckling loads of multilayered composite beams using Refined Zigzag Theory (RZT) and Higher-Order Haar Wavelet Method (HOHWM)

M. Sorrenti[a*], M. Di Sciuva[a], J. Majak[b], F. Auriemma[b]

[a] Department of Mechanical and Aerospace Engineering – Politecnico di Torino, Corso Duca degli Abruzzi 24, 10129, Torino, Italy, marco.disciuva@polito.it – matteo.sorrenti@polito.it

[b] Department of Mechanical and Industrial Engineering - Tallinn University of Technology, Tallinn, Estonia juri.majak@talctech.ee - fabio.auriemma@taltech.ee

Abstract

The paper presents a review of Haar Wavelet Methods and an application of the Higher-Order Haar Wavelet Method to study static and buckling loads of multilayered composite beams. Refined Zigzag Theory (RZT) is used to formulate the governing differential equations (equilibrium/stability equations and boundary conditions). This theory is based on the superposition of a global first-order kinematic and local layer-wise correction of the in-plane displacements. To solve numerically the set of governing differential equations, the recently developed Higher-Order Haar Wavelet Method (HOHWM) is used. This method uses the Haar wavelet expansion to approximate the derivatives of the unknown kinematic variables that form the equilibrium equations. Static and buckling load results are compared with those obtained by applying the widely used Haar Wavelet Method (HWM) and the Generalized Differential Quadrature Method (GDQM). The relative numerical performances of these numerical methods are assessed and validated against the exact analytical solution. Furthermore, a detailed convergence study is conducted analyzing the convergence characteristics (absolute errors and order of convergence) of the method presented. It is concluded that the HOHWM, when applied to RZT beam equilibrium equations for static and linear buckling problems, is capable of predicting with good accuracy the unknown kinematic variables and their derivatives with relatively few points. The HOHWM is also computationally competitive with the other compared numerical methods.

* Corresponding Author: Matteo Sorrenti, email: matteo.sorrenti@polito.it Tel. +39 3337120343.

1. Introduction

In the last decades, multilayered structures have been widely used in various engineering fields (automotive, aerospace, marine, civil, military, etc.). Their extensive use in different applications is due to excellent specific properties, high stiffness-to-weight and strength-to-weight ratio. On the other hand, some drawbacks (typically of multilayered composite structures), i.e. transverse shear deformability and transverse anisotropy, need to be accurately described in order to correctly predict the structural response.

The most common approaches used to analyze these structures are based on some kinematic assumptions that lead to a displacement field. Among these axiomatic theories, the widely used ones are the Equivalent Single Layer (ESL) theories, in which the displacement field is assumed smoothly continuous through-the-thickness, regardless of the number of layers. ESL theories generally provide accurate global result quantities such as transverse displacements, vibrational frequencies and critical buckling loads, but they often produce inaccurate through-the-thickness distributions of in-plane displacements, strains and stresses. Especially in multilayered structures, the ESL theories are not capable of predicting accurately transverse shear strains and stresses, responsible for damage and interlaminar failures. The Bernoulli-Euler Theory (BET) cannot predict accurate results for thick beams. The Timoshenko Beam Theory (TBT) is more accurate than BET, but it requires an additional shear correction factor to correct the approximated values for an uncorrected transverse shear stress distribution. The Higher-Order theories, like the Reddy's Third Order Theory, are accurate and can predict the parabolic distribution of transverse shear stress but they show some inconsistencies for some boundary conditions, i.e null transverse shear stress distribution at the clamped edge. Moreover, the transverse shear stress continuity is not satisfied. Nevertheless, such theories due to their low computational cost are very attractive and widely used in Finite Element commercial codes. For a more detailed review of these theories, the reader is addressed to the review of Abrate and Di Sciuva [1].

An alternative approach to the ESL theories is represented by the Layer-Wise (LW) theories, in which a displacement field is assumed independently for each layer and the compatibility conditions are imposed at the interfaces. The most interesting aspect of LW theories is that they can produce more accurate predictions for displacements and stresses than ESL theories. However, the computational cost is as expensive as the number of layers is higher, thus these methods become prohibitive for composite beam with several number of layers. The reader interested in these topics is addressed to see the works of Liew et al. [2] and Abrate and Di Sciuva [3].

It is commonly accepted that a good compromise between the accurate, but computationally expensive, LW theories and the less accurate, but computationally less expensive, ESL theories, is

given by the so-called zigzag theories (ZZT). In such theories, the typical zigzag distribution of in-plane displacements shown for a multilayered structure is obtained by a superposition of a general through-the-thickness polynomial distribution, such as the ESL theories, and a piecewise linear continuous function called local or zigzag contribution. As a result of this approach, the kinematic of ZZT has a fixed number of unknown variables, that not depends on the number of layers (like the ESL theories). At the same time, they provide more accurate results (generally comparable with the LW theories), maintaining reduced computational costs. The first researches on ZZT are represented by the work of Di Sciuva [4–6], Murakami [7], Cho and Parmerter [8].

Recently, a new refined zigzag theory (RZT) has been developed by Tessler and co-workers [9–11] in order to analyze multilayered composite and sandwich structures (beams, plates and shells). This RZT has some great advantages compared to the previous zigzag theories: it requires only C^0 continuity in the finite element formulation (FEM), that makes it very attractive from a computational point of view, differently from the classical Di Sciuva's ZZT that requires C^1 continuity; no shear correction factors are required and there are no inconsistency on the transverse shear stress distributions at clamped edges. The reliability and accuracy of RZT to predict the structural behavior of multilayered composite and sandwich beams have deeply investigated by various researchers. Gherlone et al. [12] a and Oñate et al. [13] developed and assessed various RZT beam elements to analyze the static behavior of composite beams. Furthermore, Eijo et al. [14] used the RZT beam elements to model and study the delamination in composite laminated beam structures. In Gherlone [15], a comparison between the results obtained using different zigzag functions has been made with particular attention to the effect of external weak layers. Di Sciuva et al. [16], on the basis of RZT specialized for beam structures, developed higher-order finite elements guaranteeing accurate results for the kinematic variables and their derivatives. The accuracy of RZT to predict the through-the-thickness transverse shear stress distributions has been further increased by using the Reissner's Mixed Variational Theorem (RMVT) [17–20] in which the transverse shear continuity is satisfied a priori. Moreover, RZT has been also used to study the timber beam structures with interlayer slip by Wimmer et al [21,22]. A recent application of RZT and perydinamic differential operator to study the stresses of laminated composite beams has be done by Dorduncu [23]. RZT has been also successfully applied to static, stability and free vibration analyses of functionally graded structures [24,25]. The accuracy of RZT has also been demonstrated by Ascione and Gherlone [26] to study the non-linear static analysis of sandwich beams, in which the RZT-FEM solution has been compared with the high fidelity FE codes.

In the above research works, different numerical methods have been used to solve the system of differential equation in terms of unknown kinematic variables. The eight-order system of ordinary

differential equations, with constant coefficients, given by RZT theory, can be solved exactly for some simplest cases with the Navier's method or integrating the equations using the standard technique for ordinary differential equations as is shown in Tessler et al. [9]. In the previously mentioned literature review on RZT, other approximated methods have been used, such as the finite element method [12], the Ritz method [27] and the perydinamic differential operator [23].

Recently, a new numerical approach has been increasingly used to solve the governing equations for beam structures. This method is the Haar Wavelet Method (HWM). The HWM introduced by Chen and Hsiao [28] has been used to solve lumped and distributed parameter system problems. This method has been assessed and used to solve a wide range of differential, integro-differential, as well as integral equations [29–34]. Moreover, the HWM has been used to solve also some structural problems such as free vibration analysis of cylindrical shells [35] and functionally graded conical shells and annular plates [36]. The HWM has been applied also to elastodynamic problems of orthotropic plates and shells by Majak et al. [37] and in the detection of delamination in conjunction with the artificial neural networks [38]. The accuracy of HWM has been accurately assessed by Majak et al. [39], and the order of convergence of the method has been studied, in Ref. [40], for various cases demonstrating to be equal to two. Further studies and comparisons on axially functionally graded beam have been made by Kirs et al. [41] considering different numerical methods. Results obtained by using HWM (for more details, see Ref. [41]) have been compared with results obtained by using widely spread methods based on strong formulation of the governing equations, i.e. the differential quadrature method (DQM), finite difference method (FDM) and the 3D solid finite element modelling. In Ref. [41] it has been concluded that the HWM needs to be improved in order to compete numerically with DQM and the other methods. Thus, the HWM has been actually improved, resulting in the newly Higher-Order-Haar-Wavelet-Method (HOHWM) [42] in which the order of convergence has been increased and the error reduced. Currently, the HOHWM has been implemented with success in recent studies [43–45].

Aim of the present investigation is to assess the relative numerical performances of the HOHWM in solving the governing equations of the static response and bucking loads of the multilayered composite beams, based on the RZT.

The present work is organized as follow.

In Section 2, the kinematic assumptions of RZT are presented. The differential equilibrium equations in terms of unknown kinematic variables for a multilayered composite beam are obtained using the principle of virtual work.

In Section 3, the main steps of the solution procedure using HOHWM are presented.

In Section 4, numerical studies are performed to critically assess the accuracy of the present method in conjunction with RZT. The static and stability behaviors are analyzed for some sample problems in which the exact analytical solution can be obtained. In order to assess the numerical merits of HOHWM, a comparison is done with the Haar Wavelet Method and the Generalized Differential Quadrature Method (GDQM).

Finally, in conclusions the main advantages of HOHWM are highlighted, with respect the other numerical methods, in the analysis of multilayered composite beams and further considerations are provided.

2. Governing equations

2.1 Geometrical preliminaries

We consider a multilayered straight beam made of a finite number N_L of perfectly bonded layers. L is the length of the beam, h the thickness, and b the width. The thickness across the beam length is assumed constant as well as the thickness of each layer. The material of each layer is assumed to be orthotropic with a plane of elastic symmetry parallel to the reference surface and whose principal orthotropy directions are arbitrarily oriented with respect to the reference frame. The points of the beam are referred to an orthogonal Cartesian co-ordinate system $\mathbf{X} = \{x_j\}$ $(j=1,2,3)$, where $\mathbf{x} = \{x_\alpha\}$ $(\alpha=1,2)$ is the set of in-plane co-ordinates on the reference plane $(x_1 \equiv x, x_2 \equiv y)$, here chosen to be the middle plane of the beam, and $x_3 \equiv z$ is the co-ordinate normal to the reference plane (see Figure 1 for the general beam notation); the origin of the reference frame is fixed at left edge of the beam, so that, x_1 is defined in the range $x_1 \in [0, +l]$, x_2 in the range $x_2 \in \left[-\frac{b}{2}, +\frac{b}{2}\right]$, and x_3 in the range $x_3 \in \left[-\frac{h}{2}, +\frac{h}{2}\right]$. If not otherwise stated, in the paper the superscript (k) is used to indicate quantities corresponding to the kth layer $(k=1,…,N_L)$, whereas the subscript (k) defines quantities corresponding to the kth interface $(k=1,…,N_L-1)$ between the k and $(k+1)$ layer. So, in the following, the symbol $(.)_{(k)}$ stands for $(.)$ valued for $x_3 = z_{(k)}$, i.e., at the k-th interface. Also, we use the subscript b and t to indicate the top and bottom surfaces of the beam; specifically, $z_{(0)} = z_b$ and $z_{(N_L)} = z_t$ denote the co-ordinates of the bottom and top surfaces of the whole beam; thus, $h = z_t - z_b$ is the beam thickness and $h^{(k)} = z_{(k)} - z_{(k-1)}$ $(k=1,2,…,N_L)$, the thickness of the kth layer (see Figure 1). The beam is acted upon by transverse distributed loads (forces per unit length) on the top $(\bar{q}_z)$ surface (see, Figure 1).

The symbol $(\bullet)_{,i} = \dfrac{\partial(\bullet)}{\partial x_i}$ refers to the derivative of the function $(\bullet)$ with respect to the coordinate x_i.

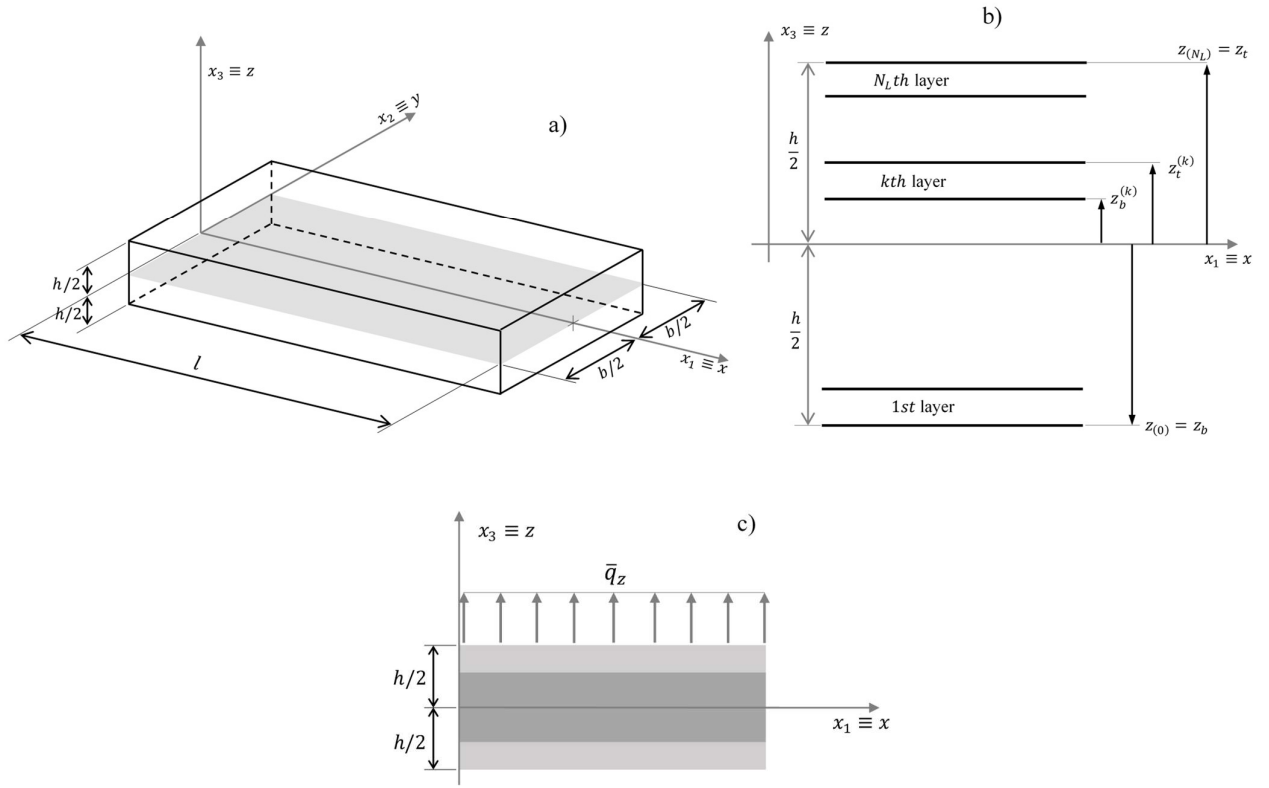Figure 1 shows the multilayered beam scheme considered in this study.

Figure 1 – General beam notation (a) beam geometry and co-ordinate system, (b) layer numbering and (c) transverse load configuration.

2.2 RZT kinematic

In this study, the kinematic of Refined Zigzag Theory is adopted [9,12]. The RZT displacement field is based on the superposition of a global (G) first–order kinematics (the one of the Timoshenko's beam theory) and a local (L) layer-wise correction of the in-plane displacements (see, Figure 2 for a detailed representation of various contributes). Thus, the displacement field is written as follows

$$\tilde{u}^{(k)}(x,z) = \tilde{u}^G(x,z) + \tilde{u}^L(x,z)$$
$$\tilde{u}_3^{(k)}(x,z) = \tilde{u}_3^G(x,z) \tag{1}$$

where

$$\tilde{u}^G(x,z) = u(x) + z\theta(x)$$
$$\tilde{u}_3^G(x,z) = w(x) \tag{2}$$

gives the contribution, which is continuous with its first derivatives with respect to the z-coordinate and

$$\tilde{u}^{L(k)}(x,z) = \phi^{(k)}(z)\psi(x) \tag{3}$$

gives the contribution to the axial displacement, which is continuous with respect to z, but with jumps in the first derivative at the interfaces between adjacent layers.

In the previous equations, u is the uniform displacement along the $x-$ axis (coincident to that of a point belonging to the longitudinal axis of the beam, for symmetric laminate); θ is the bending rotation of the normal to the beam axis along the directions $+x_2$, and w is the transverse deflection, assumed to be constant along the thickness; ψ represents the spatial amplitudes of the zigzag functions $\phi^{(k)}$. It should be noted that Timoshenko's beam theory (TBT) is a special case of the RZT, i.e. when in Eq. (1) $\tilde{u}^{L(k)} = 0$.
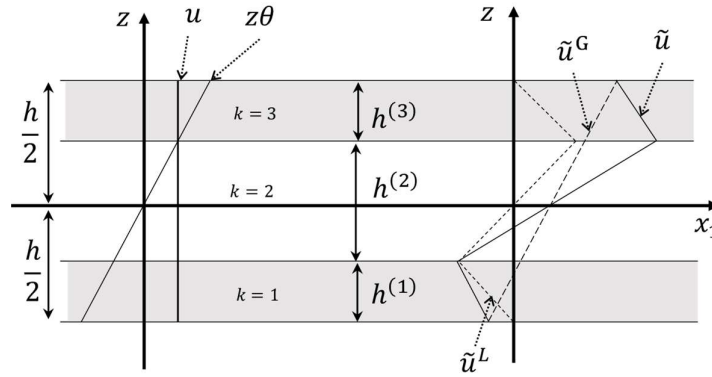

Figure 2 – Contributions to the in-plane RZT kinematic for a three-layered laminate.

2.3 Strain-displacement and constitutive relations

The linear strain expressions associated with the displacement field in Eq. (1) are the followings

$$\tilde{\varepsilon}_x^{(k)} = \varepsilon_m + z\varepsilon_b + \phi^{(k)}\varepsilon_\phi \tag{4}$$

$$\tilde{\gamma}^{(k)} = \gamma^{(0)} + \phi_{,3}^{(k)}\psi = \gamma^{(0)} + \beta^{(k)}\psi \tag{5}$$

where

$$\varepsilon_m = u_{,x}; \quad \varepsilon_b = \theta_{,x}; \quad \varepsilon_\phi = \psi_{,x}; \quad \tilde{\gamma}^{(k)} = \gamma_{xz}^{(k)} = u_{,z}^{(k)} + w_{,x}; \quad \gamma^{(0)} = \theta + w_{,x} \tag{6}$$

In order to recast the previous equations in matrix format, let us introduce the following matrices

$$\mathbf{e}^T = \begin{bmatrix} \varepsilon_m & \varepsilon_b & \varepsilon_\phi & \gamma^{(0)} & \psi \end{bmatrix} \tag{7}$$

$$\mathbf{d}^T = \begin{bmatrix} u & \theta & \psi & w \end{bmatrix} \tag{8}$$

So,

7

$$\mathbf{e} = \begin{Bmatrix} \varepsilon_m \\ \varepsilon_b \\ \varepsilon_\phi \\ \gamma^{(0)} \\ \psi \end{Bmatrix} = \begin{Bmatrix} u_{,x} \\ \theta_{,x} \\ \psi_{,x} \\ \theta + w_{,x} \\ \psi \end{Bmatrix} = \begin{bmatrix} (.)_{,x} & 0 & 0 & 0 \\ 0 & (.)_{,x} & 0 & 0 \\ 0 & 0 & (.)_{,x} & 0 \\ 0 & 1 & 0 & (.)_{,x} \\ 0 & 0 & 1 & 0 \end{bmatrix} \begin{Bmatrix} u \\ \theta \\ \psi \\ w \end{Bmatrix} \tag{9}$$

In compact matrix format,

$$\mathbf{e} = \nabla \mathbf{d} \tag{10}$$

For the kth layer of thickness $h^{(k)}$, the refined zigzag functions have the following expressions [15]:

$$\phi^{(1)}(z) = \left(z + \frac{h}{2} \right)\left(\frac{Q_4}{\overline{Q}_{44}^{(1)}} - 1 \right) \quad (k=1)$$

$$\phi^{(k)}(z) = \left(z + \frac{h}{2} \right)\left(\frac{Q_4}{\overline{Q}_{44}^{(k)}} - 1 \right) + \sum_{q=2}^{k} h^{(q-1)}\left(\frac{Q_4}{\overline{Q}_{44}^{(q-1)}} - \frac{Q_4}{\overline{Q}_{44}^{(k)}} \right) \quad (k=2,...,N_L)$$

$$\tag{11}$$

where

$$Q_4 = \left(\frac{1}{h} \sum_{k=1}^{N_L} \int_{z_b^{(k)}}^{z_t^{(k)}} \frac{dz}{\overline{Q}_{jj}^{(k)}} \right)^{-1} \tag{12}$$

and $\overline{Q}_{44}^{(k)}$ is the transformed reduced transverse shear stiffness modulus of the kth layer.

The constitutive equations for a generally orthotropic layer are

$$\tilde{\sigma}_x^{(k)} = \overline{Q}_{11}^{(k)} \tilde{\varepsilon}_x^{(k)}; \qquad \tilde{\tau}_{xz}^{(k)} = \overline{Q}_{44}^{(k)} \tilde{\gamma}_{xz}^{(k)} \tag{13}$$

where $\overline{Q}_{11}^{(k)}$ and $\overline{Q}_{44}^{(k)}$ are the transformed plane stress reduced stiffness moduli of the kth layer.

2.4 Equilibrium equations and boundary conditions in terms of stress resultants

The equilibrium equations can be derived using the principle of virtual work, defined as follows:

$$\delta U - \delta W_{ext} = 0 \tag{14}$$

where δ is the variational operator, δU is the work done by internal forces (stresses) and δW_{ext} is the virtual work done by the applied forces.

The virtual work done by the internal stresses can be expressed as

$$\delta U = \int_0^l \int_S \left(\delta \tilde{\varepsilon}_x^{(k)} \tilde{\sigma}_x^{(k)} + \delta \tilde{\gamma}_{xz}^{(k)} \tilde{\tau}_{xz}^{(k)} \right) dS dx \tag{15}$$

where S stand for the area of the cross-section of the beam.

The virtual work done by the applied transverse load per unit length $\overline{q}_z$ and the virtual variation strain energy related to the applied axial compressive force $\overline{N}$ at the ends of the beam, is given by

$$\delta W_{ext} = \int_0^l \bar{q}_z \delta w \, dx + \int_0^l \bar{N} w_{,x} \delta w_{,x} \, dx \tag{16}$$

In Eq. (16), $\bar{N} = 0$ for bending analysis and $\bar{q}_z = 0$ for buckling analysis.

Substituting Eqs. (4), (5) and (13) into Eq. (15) and integrating by parts Eq. (14) yields to the following **equilibrium equations**

$$\begin{aligned}
\delta u) \quad & N_{,x} = 0 \\
\delta\theta) \quad & M_{,x} - T = 0 \\
\delta w) \quad & T_{,x} + \bar{q}_z = \bar{N} w_{,xx} \\
\delta\psi) \quad & M_{,x}^{(\phi)} - T^{(\phi)} = 0
\end{aligned} \tag{17}$$

along with the variationally consistent boundary conditions
On $x=0,l$, specify one element of the following two pairs :

$$\begin{aligned}
u \quad & \text{or} \quad N \\
w \quad & \text{or} \quad T - \bar{N} w_{,x} \\
\theta \quad & \text{or} \quad M \\
\psi \quad & \text{or} \quad M^\phi
\end{aligned} \tag{18}$$

In Eqs. (17) and (18) the following force and moment stress resultants have been introduced

$$\left(N, M, M^\phi\right) = \int_S \left(1, z, \phi^{(k)}\right) \tilde{\sigma}_x^{(k)} dS; \quad \left(T, T^\phi\right) = \int_S \left(1, \beta^{(k)}\right) \tilde{\tau}_{xz}^{(k)} dS \tag{19}$$

The **RZT beam constitutive relations** are derived by substituting the constitutive relations of Eq. (13) into the Eq. (19), and integrating over the beam cross-section S. The resulting beam constitutive relations are expressed in matrix format as follows

$$\mathbf{R} = \mathbf{Se} \tag{20}$$

where

$$\mathbf{R} = \begin{Bmatrix} N \\ M \\ M^\phi \\ T \\ T^\phi \end{Bmatrix}; \quad \mathbf{S} = \begin{bmatrix} A & B & A^\phi & 0 & 0 \\ B & D & B^\phi & 0 & 0 \\ A^\phi & B^\phi & D^\phi & 0 & 0 \\ 0 & 0 & 0 & A_\tau & B_\tau \\ 0 & 0 & 0 & B_\tau & D_\tau \end{bmatrix} \tag{21}$$

and

$$\begin{aligned}
&\left(A, B, D\right) = \left\langle b(z)(1, z, z^2) \bar{Q}_{11}^{(k)} \right\rangle, \quad \left(A^\phi, B^\phi, D^\phi\right) = \left\langle b(z)\left(1, z, \phi^{(k)}\right) \phi^{(k)} \bar{Q}_{11}^{(k)} \right\rangle \\
&\left(A_\tau, B_\tau, D_\tau\right) = \left\langle b(z)\left(1, \beta^{(k)}, \beta^{(k)2}\right) \bar{Q}_{44}^{(k)} \right\rangle
\end{aligned} \tag{22}$$

9

In Eq. (22), $b(z)$ is the width of beam cross section that for generality is assumed to be variable along the z-axis. Moreover,

$$\langle ... \rangle = \sum_{s=1}^{N_L} \int_{z^{(s-1)}}^{z^{(s)}} (...)dz \tag{23}$$

2.5 Equations of motion and boundary conditions in terms of generalized displacements

Substituting the beam constitutive relations (20) inside the equilibrium equations expressed in terms of forces and bending moments, Eq.s (17), the same equations can be rewritten in terms of generalized displacements as follows

$$\begin{aligned}
\delta u) \quad & Au_{,xx} + B\theta_{,xx} + A^\phi \psi_{,xx} = 0 \\
\delta\theta) \quad & Bu_{,xx} + D\theta_{,xx} + B^\phi \psi_{,xx} - A_\tau\left(\theta + w_{,x}\right) - B_\tau \psi = 0 \\
\delta w) \quad & A_\tau \theta_{,x} + A_\tau w_{,xx} + B_\tau \psi_{,x} = -\bar{q}_z + \bar{N}w_{,xx} \\
\delta\psi) \quad & A^\phi u_{,xx} + B^\phi \theta_{,xx} + D^\phi \psi_{,xx} - B_\tau \theta - B_\tau w_{,x} - D_\tau \psi = 0
\end{aligned} \tag{24}$$

with the boundary conditions given by Eq. (18) together with the constitutive equations (20) for the mechanical boundary conditions.

3. The fundamentals of Higher-Order Haar Wavelet Method (HOHWM)

The numerical solution is based on the Higher-Order Haar Wavelet Method (HOHWM). Here below, a summary of the main steps is given. For more details of the method, the reader is encouraged to refer to a detailed description of this method, see Refs [42,45].

Let us consider the n-th order ordinary differential equation as sample,

$$G(x,u,u',u'',...,u^{(n-1)},u^{(n)}) = 0 \tag{25}$$

According to Ref. [42], the Higher-order Haar wavelet expansion is expressed as

$$\frac{d^{n+2s}u(x)}{dx^{n+2s}} = \sum_{i=1}^{\infty} a_i h_i(x), \qquad s = 1,2,... \tag{26}$$

In Eq. (26), $h_i(x)$ and a_i are the Haar functions and coefficients, respectively (see details in Ref. [42]). n is the order of the highest derivative included in the differential equation. In the simplest case, where $s = 1$, the derivative of order $n+2$ is expanded into Haar wavelets.

Integrating Eq. (26) $n+2$ times with respect to x, the resulting expression of the general unknown variable u, can be written as follows

$$u(x) = \frac{a_1 x^{n+2s}}{(n+2s)!} + \sum_{j=0}^{\infty} \sum_{k=0}^{2^j-1} a_{2^j+k+1} P_{n+2s,2^j+k+1}(x) + S_{BT}(x) + H_{BT}(x) \tag{27}$$

where $S_{BT}(x)$ and $H_{BT}(x)$ stand for the boundary conditions terms, given as

$$S_{BT}(x) = \sum_{r=0}^{n-1} c_r \frac{x^r}{r!} \tag{28}$$

$$H_{BT}(x) = \sum_{r=n}^{n+2s-1} c_r \frac{x^r}{r!} \tag{29}$$

As described in Ref. [42], the higher-order wavelet expansion as expressed by Eq. (26), does not lead to improved accuracy. The accuracy of the solution significantly depends on the conditions used for determining the integration constants. From Eqs. (28) and (29), n integration constants are determined using the boundary conditions and the remaining $2s$ constants require to use an appropriate procedure. Herein, two algorithms can be used to compute the integration constants of Eq. (27) as referenced by Majak et al. [42]; the first one is based on using uniform grid points and the second one uses the Selected Chebyshev–Gauss–Lobatto grid points. In this case, the simplest approach for HOHWM, i.e. with the parameter $s=1$ in Eq.(26), the exposed two main algorithms for determining complementary integrations constants coincide. Thus, the two complementary integration constants are determined by satisfying the differential equation in the boundary points, in addition to the collocation points.

4. Numerical results

In this section, numerical results on bending, and buckling under axial compressive end-load of a beam with symmetric rectangular cross-section are presented. In order to assess the reliability of the High Order Haar Wavelet Method (HOHWM) in conjunction with RZT, several numerical comparisons are made.

For a symmetric rectangular cross-section, the equilibrium equations (24) in terms of generalized displacements can be further simplified, resulting

$$D\theta_{,xx} + B^\phi \psi_{,xx} - A_\tau \left(\theta + w_{,x} \right) - B_\tau \psi = RHS_\theta \tag{30}$$

$$A_\tau \theta_{,x} + A_\tau w_{,xx} + B_\tau \psi_{,x} = RHS_w \tag{31}$$

$$B^\phi \theta_{,xx} + D^\phi \psi_{,xx} - B_\tau \theta - B_\tau w_{,x} - D_\tau \psi = RHS_\psi \tag{32}$$

where the RHS of the equilibrium equations reads for the different cases:

P1a) Bending under sinusoidal pressure ($\bar{q}_z$) and simply supported boundary conditions

$$RHS_\theta = 0; \qquad RHS_w = -\bar{q}_0 \sin\frac{\pi}{l} x; \qquad RHS_\psi = 0.$$

11

P1b) Bending under tip load (F) and clamped-free boundary conditions

$$RHS_\theta = 0; \qquad RHS_w = 0; \qquad RHS_\psi = 0.$$

P2a) Buckling under axial compressive end-load ($\bar{N}$) and simply supported boundary conditions

$$RHS_\theta = 0; \qquad RHS_w = \bar{N}w_{,xx}; \qquad RHS_\psi = 0.$$

In our numerical investigation, we consider the following boundary conditions:

a) Simply-supported at $x=0,l$

$$w = M = M^\phi = 0$$

where $M = D\theta_{,x} + B^\phi\psi_{,x}; \quad M^\phi = B^\phi\theta_{,x} + D^\phi\psi_{,x}$

b) Cantilever beam under transverse tip load F

$x=0$) Clamped end $\quad w = \theta = \psi = 0;$

$x=l$) Free end $M = M^\phi = 0; \quad T = F$.

Figure 3 shows a schematic representation of previous load configurations and boundary conditions considered in this analysis.
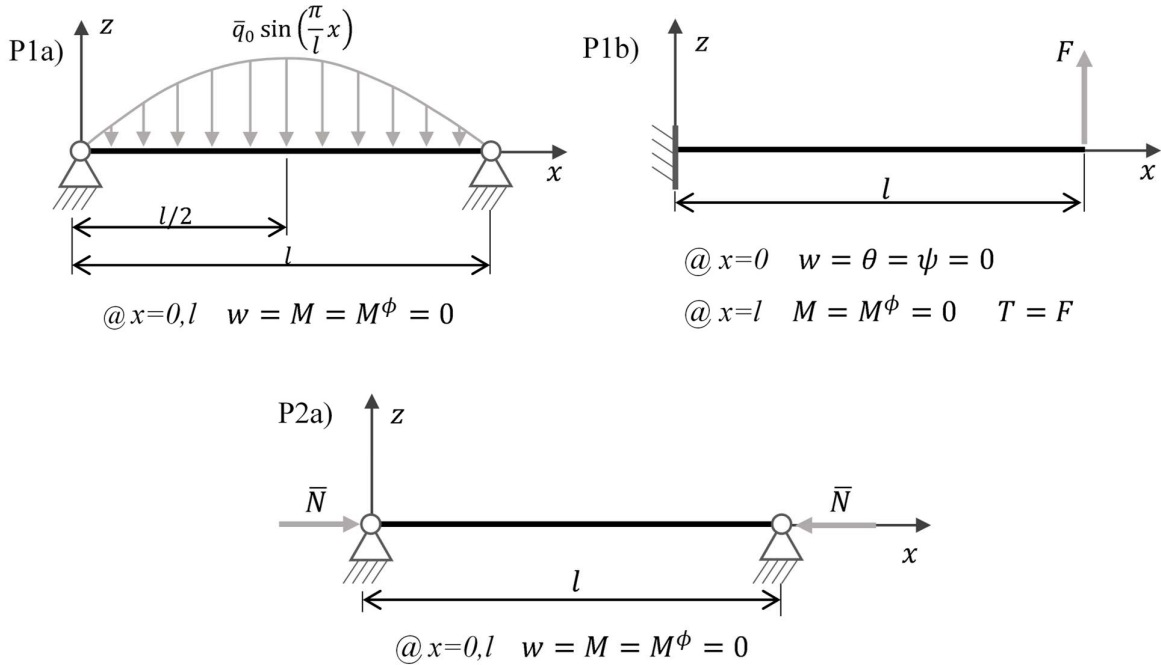

Figure 3 – Beam dimensions, boundary conditions and load configurations: P1a) simply supported under transverse sinusoidal pressure, P1b) cantilever beam under transverse tip load F and P2a) simply supported under axial compressive end forces $\bar{N}$.

The material considered in this analysis is Carbon/Epoxy, and their mechanical properties are expressed in Table 1. In Table 2 is shown the laminate stacking sequence from bottom to the top surface.

Table 1 – Mechanical properties of Carbon/Epoxy material used

Material Name	E_1 (MPa)	E_2 (MPa)	E_3 (MPa)	G_{12} (MPa)	G_{13} (MPa)	G_{23} (MPa)	ν_{12}	ν_{13}	ν_{23}	$\rho\left(\frac{Kg}{m^3}\right)$
CE	110000	7857	7857	3292	3292	1292	0.33	0.33	0.49	1600

Table 2 – Laminate stacking sequences (from bottom to top surface)

Laminate Name	$h^{(k)}/h$	Lamina orientation [°]	Materials
B	$\frac{1}{3}/\frac{1}{3}/\frac{1}{3}$	0/90/0	CE/CE/CE

The non-dimensional quantities defined in this paper, if not otherwise specified, are defined as follows

$$\bar{u} = \frac{E_2 h^2}{q_0 l^3} u; \qquad \bar{w} = 100 \frac{E_2 h^3}{q_0 l^4} w; \qquad \bar{\sigma}_x = \frac{h^2}{q_0 l^2} \sigma_x; \qquad \bar{\tau}_{xz} = \frac{h}{q_0 l} \tau_{xz} \tag{33}$$

In the remaining part of the paper, the "Analytical solution" acronym refers to the RZT solution obtained solving analytically the equilibrium equations (30)-(32). For simply supported bending and buckling analyses the Navier-type solution has been used (Ref. [46]), for cantilever beam under transverse tip load the analytic solution of Ref. [9] has been used. The order of convergence (*OC*) can be computed using the following formula (Ref. [40])

$$OC = \frac{\log\left(\dfrac{V_{i-1} - V_{analytic}}{V_i - V_{analytic}}\right)}{\log(2)} \tag{34}$$

where V_i is the computed value at *i*th step, V_{i-1} is the computed value at *(i-1)*th step and $V_{analytic}$ the exact analytical computed value. The absolute error is computed as follow

$$err = \left|V_{numeric} - V_{analytic}\right|$$

where $V_{numeric}$ is the numeric solution using one of the numerical method considered in this paper, and $V_{analytic}$ is the solution using the analytical method. If not otherwise specified, the parameter *s=1* expressed in Eq.(26) is used to solve our numerical problems, thus the two algorithms are coincident and an uniform grid points is used.

4.1 Bending problem

In this first analysis, we consider two simple problems: a simply supported beam under sinusoidal transverse pressure (Problem P1a) and a cantilever beam under tip load (Problem P1b). For these cases, the span-to-thickness ratio here considered is $l/h=1$ (thick beam). We also consider the width of beam $b=1$mm.

In order to assess the accuracy of the HOHWM in conjunction with RZT in Table 3 is shown the convergence analysis for the non-dimensional maximum deflection of a simply supported beam under sinusoidal transverse pressure, where N_P is the number of collocation points used in the present method. For comparison purpose, in Table 3 are also shown the results using the Haar Wavelet Method (HWM) developed by Chen and Hsiao [28] in conjunction with RZT.

Table 3 – Convergence analysis for non-dimensional maximum deflection using the HOHWM and RZT.

N_P	Present method (HOHWM)			HWM [28]			Error ratio
	$\overline{w}$	Absoslute error	Order of convergence	$\overline{w}$	Absoslute error	Order of convergence	
4	34.762379179	4.35E-02		34.009910998	7.96E-01		18.3
8	34.803324480	2.53E-03	4.1027	34.618821536	1.87E-01	2.0894	73.9
16	34.805699567	1.55E-04	4.0256	34.759825451	4.60E-02	2.0227	296.2
32	34.805845274	9.67E-06	4.0064	34.794392842	1.15E-02	2.0057	1185.6
64	34.805854339	6.04E-07	4.0016	34.802992242	2.86E-03	2.0014	4742.7
128	34.805854904	3.77E-08	4.0000	34.805139444	7.15E-04	2.0004	18966.0
256	34.805854939	3.14E-09	3.5871	34.805676079	1.79E-04	2.0001	56979.1
512	34.805854940	1.91E-09	0.7166	34.805810227	4.47E-05	2.0000	23408.6
1024	34.805854945	3.20E-09	-0.7447	34.805843763	1.12E-05	2.0000	3492.5
Analytical solution			**34.805854942**				

It can be observed from the last column of Table 3 that the error of the widely used HWM is 18 up to 18966 times bigger than of the HOHWM. The accuracy achieved by HWM using mesh 1024 (collocation points) is achieved by applying HOHWM in the case of 32 collocation points. Furthermore, the order of convergence tends to 2 in the case of HWM and to 4 in the case of HOHWM as confirmed by Majak et al. [42,44,45]. As expected, in the case of HOHWM, the limit of double-

precision computing is reached with N_P =256, thus further increasing of mesh will lead to reduced accuracy.

The accuracy of HOHWM to compute the other kinematic variables and their derivatives is evaluated comparing the strain and stress distributions in some points along the beam. The HOHWM results are obtained using N_P=256 collocation points.
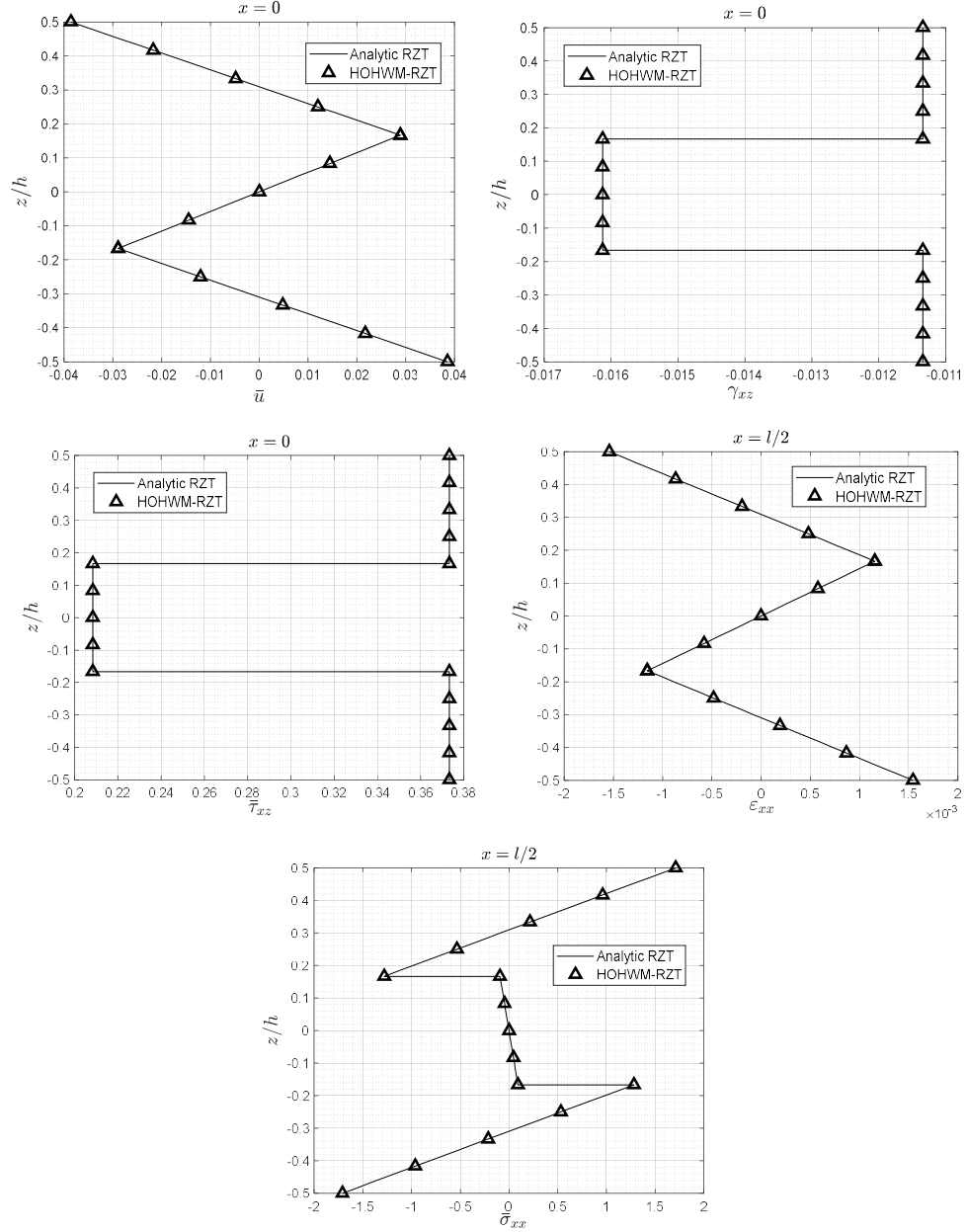

Figure 4 – Comparison between analytic and HOHWM-RZT results for through-the-thickness distribution of in-plane displacement, strains and stresses at various point of simply supported beam (problem P1a)
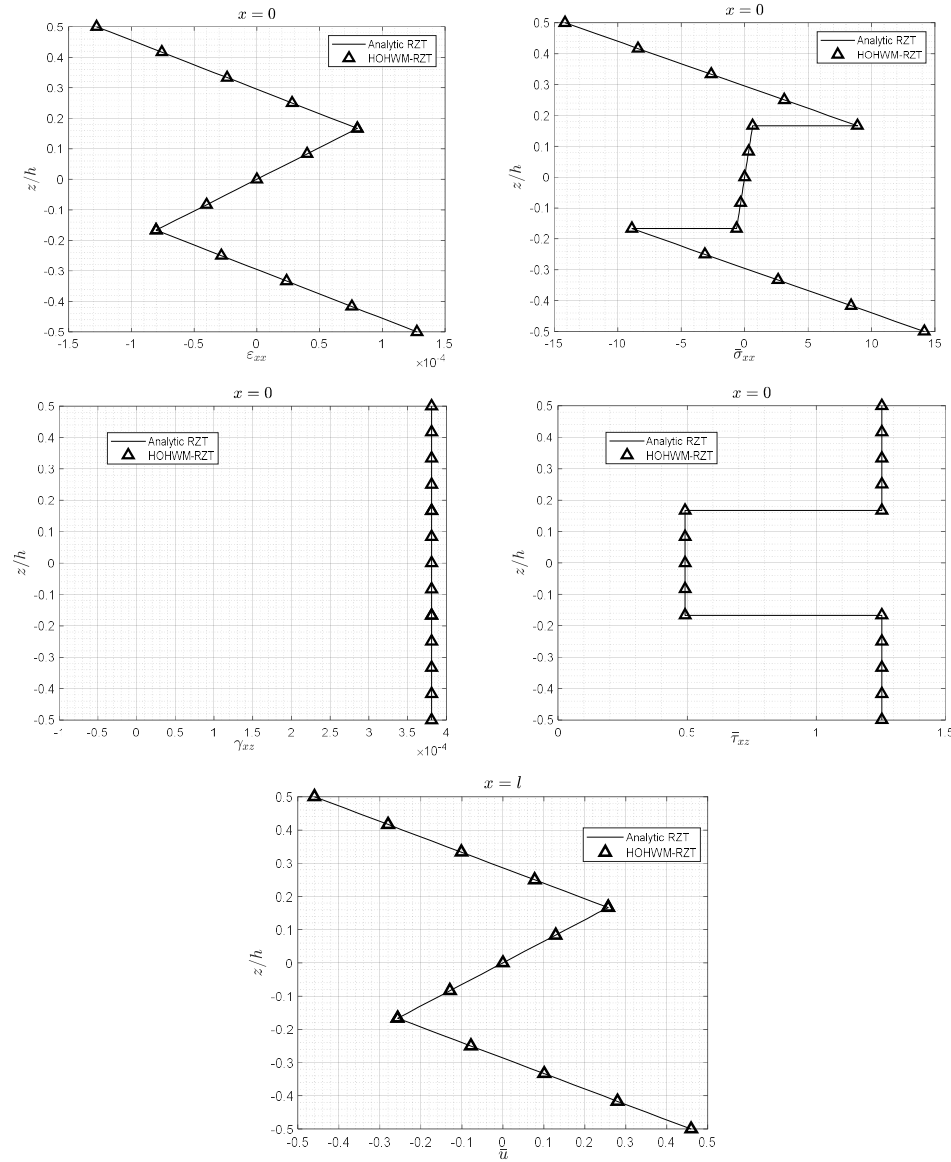
Figure 5 - Comparison between analytic and HOHWM-RZT results for through-the-thickness distribution of in-plane displacement, strains and stresses at various point of cantilever beam (problem P1b). In this case, the non-dimensional expressions use $q_0 = F/l$.

Figure 4 and Figure 5 reveal the ability of HOHWM to compute the kinematic variables and their derivatives, which are necessary to obtain the through-the-thickness distributions typical for a three-layered beam using RZT. As can be seen from Figure 4 and Figure 5, the solution obtained by applying HOHWM (s=1) is in good agreement with the analytic one.

One of the most accurate strong formulation numerical method widely used in the open literature is the Generalized Differential Quadrature Method (GDQM) [41,47–51]. This method is based on the use of high order polynomials and typically achieves excellent accuracy. Some shortcomings of the GDQM known are low accuracy with coarse mesh and problems with finer mesh. A comparison of

HOHWM in conjunction with RTZ is made with the GDQM. In Table 4 the HOHWM ($s=2$) and GDQM results for maximum deflection of a simply supported beam under sinusoidal load (problem P1a) are compared.

Table 4 – Comparison between convergence analysis for non-dimensional maximum deflection (problem P1a): HOHWM ($s=2$) and GDQM.

	Present Method (HOHWM)			GDQM		
N_P	$\overline{w}$	Absoslute error	Order of convergence	$\overline{w}$	Absoslute error	Order of convergence
4	34.804771336088	1.08E-03		30.779603526824	4.03E+00	
8	34.805838045983	1.69E-05	6.0030	34.805242348179	6.13E-04	12.6822
16	34.805854679113	2.63E-07	6.0053	34.805854942158	3.06E-12	27.5757
32	34.805854938054	4.10E-09	6.0033	34.805854942158	3.06E-12	-0.0000
64	34.805854942025	1.30E-10	4.9806	34.805854942150	4.80E-12	-0.6472
Analytical solution			34.805854942154			

As expected, the order of convergence of the HOHWM ($s=2$) is six (see Table 4). In case of GDQM, the first two values of the order of convergence are very high but it quickly become negative at increasing of N_P (reduction of accuracy). Such behaviour is common for GDQM [41,47–49]. It can be observed from Table 4 that in the case of small mesh (N_P =4 and N_P =8), the absolute error of the HOHWM is less than that of GDQM. In the case of finer mesh (N_P =16, 32, 64) the absolute error of the GDQM is smaller. Note that in the case of GDQM, the loss of accuracy starting already from N_P =32. The latter fact may cause problems with covering local behaviour of the solution. In the case of HOHWM, an uniform mesh is used and in the case of GDQM a non-uniform mesh, based on Chebyshev–Gauss–Lobatto points, has been considered.

4.2 Buckling problem

In this section, the buckling problem of simply supported beam is considered. In the same way, we assess the accuracy of the HOHWM in conjunction with RZT for computing the critical buckling force. Similarly to the previous static bending case, the span-to-thickness ratio here considered is $l/h=1$ (thick beam) and the width of beam $b=1$mm.

In Table 5, the convergence analysis for the first critical buckling force is shown. For comparison purpose, in Table 5 are also shown the results using the Haar Wavelet Method (HWM) developed by Chen and Hsiao [28] in conjunction with RZT. Table 5 also includes the order of convergence values and the absolute errors for each number of collocation point used.

Table 5 – Convergence analysis for critical buckling load using the HOHWM and RZT.

N_P	Present method (HOHWM)			HWM [28]			Error ratio
	N_{crit} [N]	Absoslute error	Order of convergence	N_{crit} [N]	Absoslute error	Order of convergence	
4	2287.546315	3.43E-01		2293.066739	5.86E+00		17.1
8	2287.224008	2.11E-02	4.0271	2288.732707	1.53E+00	1.9385	72.5
16	2287.204256	1.31E-03	4.0074	2287.589212	3.86E-01	1.9856	294.7
32	2287.203028	8.17E-05	4.0019	2287.299750	9.68E-02	1.9965	1184.8
64	2287.202952	5.11E-06	4.0005	2287.227162	2.42E-02	1.9991	4735.8
128	2287.202947	3.19E-07	3.9987	2287.209002	6.05E-03	1.9998	18965.5
256	2287.202947	5.96E-09	5.7448	2287.204461	1.51E-03	1.9999	253355.7
512	-	-	-	2287.203325	3.78E-04	2.0000	-
1024	-	-	-	2287.203041	9.46E-05	2.0000	-
Analytical solution			**2287.202947**				

Table 5 shows that the error ratio of the widely used HWM is 17 up to 253355 times bigger that of the HOHWM. Like the static problem, the accuracy achieved by HWM using mesh 1024 (collocation points) is achieved by applying HOHWM in the case of 32 collocation points only. The numerical order of convergence tends to 2 in the case of HWM and to 4 in the case of HOHWM, which confirms the previous static results. As expected in the case of HOHWM, the limit of double precision computing is reached with N_P =256, thus further increasing of mesh will lead to reduced accuracy and negative convergence rates.

Table 6 shows the convergence analysis for the first four buckling critical loads of simply supported beam.

Table 6 - Convergence analysis for the first four buckling critical loads of simply supported beam (problem P2a).

N_P	N_{crit}^1 [N]	N_{crit}^2 [N]	N_{crit}^3 [N]	N_{crit}^4 [N]
4	2287.546315	2522.723160	2580.990931	2596.649113
8	2287.224008	2520.626692	2576.870636	2598.049786
16	2287.204256	2520.499433	2576.548143	2597.452619
32	2287.203028	2520.491625	2576.528614	2597.416282
64	2287.202952	2520.491140	2576.527407	2597.414053
128	2287.202947	2520.491109	2576.527332	2597.413914
256	2287.202947	2520.491108	2576.527327	2597.413905
Analytical solution	**2287.202947**	**2520.491107**	**2576.527327**	**2597.413905**

Table 6 shows that the HOHWM provides a very good accuracy, with relatively few collocation points, in the computation of the first four critical buckling loads. Also, high accuracy is achieved already with small meshes (N_P =4 or N_P =8).

5. Conclusions

This research study is focused on the use of the High Order Haar Wavelet Method (HOHWM) to solve the governing equation of multilayered composite beams for static and buckling analysis using the Refined Zigzag Theory (RZT). In RZT a global first-order kinematic is combined with a local layer-wise correction of the in-plane displacements to better describe the through-the-thickness behavior. In the RZT, the Timoshenko's beam theory (TBT) is verified as a particular case and the theory does not require any shear correction factors. Once the equilibrium equations for bending and buckling problems are determined by means of the RZT, the HOHWM is used to solve them.

The numerical analysis has been performed comparing the HOHWM results with the Haar Wavelet Method (HWM) ones, revealing for both static and buckling problems the high order of convergence of HOHWM with relatively few collocation points. Moreover, the same accuracy of HOHWM can be obtained by HWM with more collocation points (generally, the HWM uses 512 collocation points versus the HOHWM which uses 16 or 32 points). Furthermore, using HOHWM with the method parameter $s=2$, the same accuracy can be achieved by means of 8 collocation points only and the order of convergence is further increased up to six.

A further comparison has been made between the HOHWM ($s=2$) and the Generalized Differential Quadrature Method (GDQM). Although the GDQM has a greater order of convergence than HOHWM, especially for coarse meshes, the GDQM fails to determine the unknowns using finer meshes. The HOHWM reaches the limit of double-precision, but it is more stable and the order of convergence is still good for finer meshes.

The unknown kinematic variables and their derivatives computed using the HOHWM are also in good agreement with their analytical counterparts; this is proved by the good matching between the through-the-thickness distributions for the static problems considered.

Furthermore, considering the buckling problem, the HOHWM is very good to predict, with high accuracy, the first four critical buckling loads without using a finer mesh.

It can be concluded that the HOHWM is a good numerical method to solve the RZT beam equilibrium equations for bending and buckling problems, with a relatively high order of convergence and high accuracy. Moreover, considering the advantages and the drawbacks of the presented methods, the HOHWM is computational competitive and can be used to solve structural problems. Further studies will see this method applied to multilayered composite plates/shells and to problems based on nonlocal theories combined with RZT.

References

[1] Abrate S, Di Sciuva M. Equivalent single layer theories for composite and sandwich structures: A review. Composite Structures 2017;179:482–94. https://doi.org/10.1016/j.compstruct.2017.07.090.

[2] Liew KM, Pan ZZ, Zhang LW. An overview of layerwise theories for composite laminates and structures: Development, numerical implementation and application. Composite Structures 2019;216:240–59. https://doi.org/10.1016/j.compstruct.2019.02.074.

[3] Abrate S, Di Sciuva M. Multilayer Models for Composite and Sandwich Structures. In: Beaumont PWR, Zweben CH, editors. Comprehensive Composite Materials II, Elsevier; 2018, p. 399–425. https://doi.org/10.1016/B978-0-12-803581-8.09885-4.

[4] Di Sciuva M. Bending, vibration and buckling of simply supported thick multilayered orthotropic plates: An evaluation of a new displacement model. Journal of Sound and Vibration 1986;105:425–42. https://doi.org/10.1016/0022-460X(86)90169-0.

[5] Di Sciuva M. An Improved Shear-Deformation Theory for Moderately Thick Multilayered Anisotropic Shells and Plates. J Appl Mech 1987;54:589–96. https://doi.org/10.1115/1.3173074.

[6] Di Sciuva M. Multilayered anisotropic plate models with continuous interlaminar stresses. Composite Structures 1992;22:149–67. https://doi.org/10.1016/0263-8223(92)90003-U.

[7] Murakami H. Laminated Composite Plate Theory With Improved In-Plane Responses. J Appl Mech 1986;53:661–6. https://doi.org/10.1115/1.3171828.

[8] Cho M, Parmerter RR. An efficient higher-order plate theory for laminated composites. Composite Structures 1992;20:113–23. https://doi.org/10.1016/0263-8223(92)90067-M.

[9] Tessler A, Di Sciuva M, Gherlone M. Refinement of Timoshenko Beam Theory for Composite and Sandwich Beams using Zigzag Kinematics. NASA/TP-2007-215086 2007:1–45.

[10] Tessler A, Di Sciuva M, Gherlone M. Refined Zigzag Theory for Laminated Composite and Sandwich Plates. NASA/TP-2009-215561 2009:1–53.

[11] Versino D, Gherlone M, Di Sciuva M. Four-node shell element for doubly curved multilayered composites based on the Refined Zigzag Theory. Composite Structures 2014;118:392–402. https://doi.org/10.1016/j.compstruct.2014.08.018.

[12] Gherlone M, Tessler A, Di Sciuva M. C^0 beam elements based on the Refined Zigzag Theory for multilayered composite and sandwich laminates. Composite Structures 2011;93:2882–94. https://doi.org/10.1016/j.compstruct.2011.05.015.

[13] Oñate E, Eijo A, Oller S. Simple and accurate two-noded beam element for composite laminated beams using a refined zigzag theory. Computer Methods in Applied Mechanics and Engineering 2012;213–216:362–82. https://doi.org/10.1016/j.cma.2011.11.023.

[14] Eijo A, Oñate E, Oller S. A numerical model of delamination in composite laminated beams using the LRZ beam element based on the refined zigzag theory. Composite Structures 2013;104:270–80. https://doi.org/10.1016/j.compstruct.2013.04.035.

[15] Gherlone M. On the Use of Zigzag Functions in Equivalent Single Layer Theories for Laminated Composite and Sandwich Beams: A Comparative Study and Some Observations on External Weak Layers. J Appl Mech 2013;80:061004-061004–19. https://doi.org/10.1115/1.4023690.

[16] Di Sciuva M, Gherlone M, Iurlaro L, Tessler A. A class of higher-order C^0 composite and sandwich beam elements based on the Refined Zigzag Theory. Composite Structures 2015;132:784–803. https://doi.org/10.1016/j.compstruct.2015.06.071.

[17] Tessler A. Refined zigzag theory for homogeneous, laminated composite, and sandwich beams derived from Reissner's mixed variational principle. Meccanica 2015;50:2621–48. https://doi.org/10.1007/s11012-015-0222-0.

[18] Groh RMJ, Weaver PM. On displacement-based and mixed-variational equivalent single layer theories for modelling highly heterogeneous laminated beams. International Journal of Solids and Structures 2015;59:147–70. https://doi.org/10.1016/j.ijsolstr.2015.01.020.

[19] Groh RM, Weaver PM, Tessler A. Application of the Refined Zigzag Theory to the Modeling of Delaminations in Laminated Composites. NASA/TM-2015-218808 2015:1–22.

[20] Iurlaro L, Gherlone M, Di Sciuva M. The (3,2)-Mixed Refined Zigzag Theory for generally laminated beams: Theoretical development and C^0 finite element formulation. International Journal of Solids and Structures 2015;73–74:1–19. https://doi.org/10.1016/j.ijsolstr.2015.07.028.

[21] Wimmer H, Gherlone M. Explicit matrices for a composite beam-column with refined zigzag kinematics. Acta Mech 2017;228:2107–17. https://doi.org/10.1007/s00707-017-1816-5.

[22] Wimmer H, Hochhauser W, Nachbagauer K. Refined Zigzag Theory: an appropriate tool for the analysis of CLT-plates and other shear-elastic timber structures. Eur J Wood Prod 2020. https://doi.org/10.1007/s00107-020-01586-x.

[23] Dorduncu M. Stress analysis of laminated composite beams using refined zigzag theory and peridynamic differential operator. Composite Structures 2019;218:193–203. https://doi.org/10.1016/j.compstruct.2019.03.035.

[24] Iurlaro L, Gherlone M, Di Sciuva M. Bending and free vibration analysis of functionally graded sandwich plates using the Refined Zigzag Theory. Jnl of Sandwich Structures & Materials 2014;16:669–99. https://doi.org/10.1177/1099636214548618.

[25] Di Sciuva M, Sorrenti M. Bending, free vibration and buckling of functionally graded carbon nanotube-reinforced sandwich plates, using the extended Refined Zigzag Theory. Composite Structures 2019;227:20. https://doi.org/10.1016/j.compstruct.2019.111324.

[26] Ascione A, Gherlone M. Nonlinear static response analysis of sandwich beams using the Refined Zigzag Theory: Journal of Sandwich Structures & Materials 2018;22:2250–86. https://doi.org/10.1177/1099636218795381.

[27] Di Sciuva M, Sorrenti M. Bending and free vibration analysis of functionally graded sandwich plates: An assessment of the Refined Zigzag Theory. Journal of Sandwich Structures & Materials 2019:1–43. https://doi.org/10.1177/1099636219843970.

[28] Chen CF, Hsiao CH. Haar wavelet method for solving lumped and distributed-parameter systems. IEE Proceedings - Control Theory and Applications 1997;144:87–94. https://doi.org/10.1049/ip-cta:19970702.

[29] Lepik Ü. Numerical solution of differential equations using Haar wavelets. Mathematics and Computers in Simulation 2005;68:127–43. https://doi.org/10.1016/j.matcom.2004.10.005.

[30] Lepik Ü. Haar wavelet method for nonlinear integro-differential equations. Applied Mathematics and Computation 2006;176:324–33. https://doi.org/10.1016/j.amc.2005.09.021.

[31]   Aziz I, Siraj-ul-Islam. New algorithms for the numerical solution of nonlinear Fredholm and Volterra integral equations using Haar wavelets. Journal of Computational and Applied Mathematics 2013;239:333–45. https://doi.org/10.1016/j.cam.2012.08.031.

[32]   Aziz I, Siraj-ul-Islam, Khan F. A new method based on Haar wavelet for the numerical solution of two-dimensional nonlinear integral equations. Journal of Computational and Applied Mathematics 2014;272:70–80. https://doi.org/10.1016/j.cam.2014.04.027.

[33]   Siraj-ul-Islam, Aziz I, Al-Fhaid AS. An improved method based on Haar wavelets for numerical solution of nonlinear integral and integro-differential equations of first and higher orders. Journal of Computational and Applied Mathematics 2014;260:449–69. https://doi.org/10.1016/j.cam.2013.10.024.

[34]   Oruç Ö. A non-uniform Haar wavelet method for numerically solving two-dimensional convection-dominated equations and two-dimensional near singular elliptic equations. Computers & Mathematics with Applications 2019;77:1799–820. https://doi.org/10.1016/j.camwa.2018.11.018.

[35]   Xie X, Jin G, Liu Z. Free vibration analysis of cylindrical shells using the Haar wavelet method. International Journal of Mechanical Sciences 2013;77:47–56. https://doi.org/10.1016/j.ijmecsci.2013.09.025.

[36]   Xie X, Jin G, Ye T, Liu Z. Free vibration analysis of functionally graded conical shells and annular plates using the Haar wavelet method. Applied Acoustics 2014;85:130–42. https://doi.org/10.1016/j.apacoust.2014.04.006.

[37]   Majak J, Pohlak M, Eerme M. Application of the Haar wavelet-based discretization technique to problems of orthotropic plates and shells. Mechanics of Composite Materials 2009;45:631–42. https://doi.org/10.1007/s11029-010-9119-0.

[38]   Hein H, Feklistova L. Computationally efficient delamination detection in composite beams using Haar wavelets. Mechanical Systems and Signal Processing 2011;25:2257–70. https://doi.org/10.1016/j.ymssp.2011.02.003.

[39]   Majak J, Shvartsman B, Karjust K, Mikola M, Haavajõe A, Pohlak M. On the accuracy of the Haar wavelet discretization method. Composites Part B: Engineering 2015;80:321–7. https://doi.org/10.1016/j.compositesb.2015.06.008.

[40]   Majak J, Shvartsman BS, Kirs M, Pohlak M, Herranen H. Convergence theorem for the Haar wavelet based discretization method. Composite Structures 2015;126:227–32. https://doi.org/10.1016/j.compstruct.2015.02.050.

[41]   Kirs M, Karjust K, Aziz I, Õunapuu E, Tungel E. Free vibration analysis of a functionally graded material beam: evaluation of the Haar wavelet method. Proceedings of the Estonian Academy of Sciences, vol. 67, 2018, p. 1. https://doi.org/10.3176/proc.2017.4.01.

[42]   Majak J, Pohlak M, Karjust K, Eerme M, Kurnitski J, Shvartsman BS. New higher order Haar wavelet method: Application to FGM structures. Composite Structures 2018;201:72–8. https://doi.org/10.1016/j.compstruct.2018.06.013.

[43]   Jena SK, Chakraverty S, Malikan M. Implementation of Haar wavelet, higher order Haar wavelet, and differential quadrature methods on buckling response of strain gradient nonlocal beam embedded in an elastic medium. Engineering with Computers 2019. https://doi.org/10.1007/s00366-019-00883-1.

[44]   Majak J, Pohlak M, Eerme M, Shvartsman B. Solving ordinary differential equations with higher order Haar wavelet method. AIP Conference Proceedings 2019;2116:330002. https://doi.org/10.1063/1.5114340.

[45]   Majak J, Shvartsman B, Ratas M, Bassir D, Pohlak M, Karjust K, et al. Higher-order Haar wavelet method for vibration analysis of nanobeams. Materials Today Communications 2020;25:101290. https://doi.org/10.1016/j.mtcomm.2020.101290.

[46]   Yang W, He D, Hu Y. A refined beam model for anisotropic nanobeams based on Eringen's differential constitutive model. Composite Structures 2018;200:771–80. https://doi.org/10.1016/j.compstruct.2018.05.130.

[47]   Torabi K, Afshari H. Generalized Differential Quadrature Method for Vibration Analysis of Cantilever Trapezoidal FG Thick Plate. Journal of Solid Mechanics 2016;8:184–203.

[48]   Tornabene F, Brischetto S, Fantuzzi N, Bacciocchi M. Boundary Conditions in 2D Numerical and 3D Exact Models for Cylindrical Bending Analysis of Functionally Graded Structures. Shock and Vibration 2016;2016:e2373862. https://doi.org/10.1155/2016/2373862.

[49]   Ghannadpour SAM, Karimi M, Tornabene F. Application of plate decomposition technique in nonlinear and post-buckling analysis of functionally graded plates containing crack. Composite Structures 2019;220:158–67. https://doi.org/10.1016/j.compstruct.2019.03.025.

[50]   Tornabene F, Viola E. 2-D solution for free vibrations of parabolic shells using generalized differential quadrature method. European Journal of Mechanics - A/Solids 2008;27:1001–25. https://doi.org/10.1016/j.euromechsol.2007.12.007.

[51]   Tornabene F, Viola E, Inman DJ. 2-D differential quadrature solution for vibration analysis of functionally graded conical, cylindrical shell and annular plate structures. Journal of Sound and Vibration 2009;328:259–90. https://doi.org/10.1016/j.jsv.2009.07.031.